Effect of Clay Dispersion on the Rheological Properties and Flammability of Polyurethane-Clay Nanocomposite Elastomers

M. Berta,[1] A. Saiani,[1] C. Lindsay,[2] R. Gunaratne[1]

[1]School of Materials, The University of Manchester, M1 7HS Manchester, United Kingdom
[2]Huntsman Polyurethanes, Everslaan 45, 3078 Everberg, Belgium

ABSTRACT: Polyurethane-clay nanocomposite elastomers were synthesized using polyol-clay blends with different levels of dispersion, which affected the final elastomer microstructure. A PU-clay microcomposite elastomer containing partially dispersed clay showed poorer mechanical and similar fire properties to the unmodified polyurethane. More complete dispersion of the clay into the polyol led to an exfoliated structure in the final elastomer. This showed a higher modulus and kept a visco-elastic behavior to higher temperature than the pristine PU. The enhancement of mechanical and thermal properties in the nanocomposite elastomer can be attributed to the degree of clay exfoliation, and this also prevented dripping during the UL 94 fire test. © 2009 Wiley Periodicals, Inc. J Appl Polym Sci 112: 2847–2853, 2009

Key words: flame retardance; microstructure; nanocomposites; polyurethanes; rheology

INTRODUCTION

Polyurethanes (PUs) are an important and versatile class of polymeric materials whose properties can be easily tailored through changing the molecular structures of the flexible segment and rigid segment. Polyurethanes possess desirable properties, such as excellent flexibility, elasticity, and damping ability but also poor thermal stability and barrier properties, which limit their applications. A previous investigation[1] has shown that a nanocomposite material of polyurethane and organic-modified montmorillonite is more thermally stable than the pure polymer. In addition to the gas barrier improvement, considerable interest in polymer nanocomposites concerns the enhancement of mechanical properties due to the high level of dispersion of the filler.[2–4] However, in spite of many extensive investigations into the physical properties (mechanical and rheological) and composite structure, the relationships between these are still only partially understood for these materials.[5–9]

The objective of the present work is the systematic investigation of the effect of clay nanodispersion on the rheology of polyurethane-clay nanocomposites and its relation to the material flammability discussed in previous publication.[1]

EXPERIMENTAL

Materials

The silicate used as reinforcement for the composites investigated was Cloisite 30B obtained from Southern Clay Products, a natural montmorillonite treated with a surfactant (shown in Fig. 1) having the chemical structure methylbis-2-hydroxyethyltallow alkyl quaternary ammonium chloride.[10] Cloisite 30B was reported both in the literature[11] and in previous work[1] to promote the exfoliated level of montmorillonite in a thermoplastic PU matrix, owing to the good compatibility between the modifier and the polyurethane polar chain segments.[12] Generally, it was proposed that the improvement of affinity between Cloisite 30B and TPU facilitated the diffusion of chains, and molecular diffusion resulted in the exfoliation of the clay.[8,11]

The polyol used was ethylene oxide (EO)-tipped polypropyleneoxide polyether namely Acclaim 4220 (15% EO tip; OH_v = 28 mg/g KOH, functionality = 2) supplied by Bayer Polymers, and it was vacuum dried before use. Triethylenediamine catalyst (DABCO Solid; Air Products) was used as received. Methylenediphenylenediisocyanate (MDI; Suprasec 3050; Huntsman Polyurethanes) was used as a 50/50 mixture of the 2,4'- and 4,4'-isomers.

$$CH_3 - \overset{\overset{\displaystyle CH_2\,CH_2OH}{|}}{\underset{\underset{\displaystyle CH_2CH_2\,OH}{|}}{N^+}} - T$$
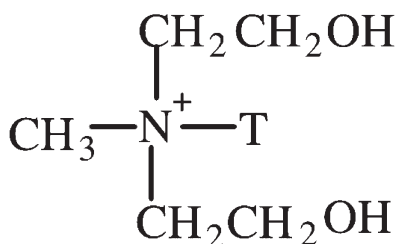
Figure 1 Quaternary ammonium salt used as modifier in Cloisite 30B; T is Tallow ($\sim$ 65% C18; $\sim$ 30% C16; $\sim$ 5% C14).[10]

Elastomer synthesis

The procedure adopted to synthesize the polyurethane-clay composite elastomers was that described more in detail previously.[1]

The desired weights of Acclaim 4220 and Cloisite 30B were measured into a 250-mL plastic beaker and two blends were mixed, one for 1 h and the other for 5 min with a high shear Silverson L4RT mixer to obtain, respectively, a good and a poor nanodispersion of the organoclay in the polyol. The polyol-clay blends were measured into another plastic cup and then placed in a Mentz degasser and subsequently stirred under high vacuum at 1000 rpm to remove any air and also, potentially, moisture from the system. After 2 h of degassing butanediol (chain extender), catalyst (DABCO S), and Suprasec 3050 (MDI) were added in appropriate amounts to generate a PU elastomer with a hard block content of $\sim$ 30% and an organoclay content of 2.5 wt %. The mixture was degassed for 1 min at 600 rpm to obtain an homogeneous and air-free solution. A mold was coated with Teflon release agent and heated on a hot plate to 120°C. The final degassed blend was rapidly poured into the mold, directly from the degasser. The PU was allowed to cure in the mold for 3 h and then it was postcured in an oven at 80°C for 24 h.

The pure PU (i.e., not modified by the addition of clay) was prepared by weighing out the desired quantities of polyol and chain extender in a plastic cup and mixing them in the degasser for 30 s. Then the isocyanate was added to obtain the same hard-block percentage, and the same curing procedure was followed as for the composite materials so that this material could be used as reference.

Experimental procedures

Wide-angle X-ray scattering (WAXS)

Data were acquired on a Philips X'Pert MPD PW3040 θ-θ system goniometer. A copper source operated at 50 kV/40 mA was used. Wavelength (Cu–Ka = 1.5418 Å) was selected through a Ni filter and automatic collimating slits were used depending on the angular range probed. Experiments were per-

formed in reflection mode. PU samples sliced from the castings were placed on a glass slide and no Lorentz-correction was applied.

Microscopy

Optical microscopy observations were made under polarized light using an Olympus optical microscope. Transmission electron microscopy was performed on ultra-microtomed sections taken from nanocomposite-PU castings using a Philips EM-301 and a Jeol JEM 2100 microscope.

DSC

Differential scanning calorimetry experiments were carried with a DSC 2100 TA apparatus. Aluminum pans containing 5–9 mg of PU elastomer were heated at 10°C/min from −80 to 250°C for two cycles under nitrogen atmosphere.

Tensile tests

Tensile strength was measured by an Instron 4301 tester at 23°C, humidity of 50%, and with crosshead speed of 50 mm/min. Tensile samples of $\approx$5 cm length and 3 mm thickness were cut out of the PU castings.

Rheology

Dynamic mechanical tensile analysis was carried out by means of a Polymer Mk II DMTA system manufactured by Rheometric Scientific. The dimensions of the samples were 3.4 × 10 × 38.6 mm. Dynamic frequency sweep tests were performed in the frequency range of ω = 0.1–5 Hz at room temperature. Temperature sweep tests were carried out in dynamic regime at frequency of 1 Hz and the temperature range considered was −135 to 200°C with a heating rate of 2°C/min. All rheological tests were conducted at constant low strain amplitude of 0.6%, because the polymer is relatively soft, using nitrogen atmosphere, to minimize thermo-oxidative degradation phenomena.

UL94 fire testing

The UL 94 vertical burn test was performed according to the ASTDM D3801 test method. In this test, a bunsen flame of controlled intensity was applied twice for 10 s to the base of test specimens of dimensions 130 × 13 × 3.2 mm and the burning behavior was observed and classified.

RESULTS AND DISCUSSION

Morphology and thermal properties

Although a homogeneous dispersion (optical scale) was obtained for the polyol-clay mixture mixed for
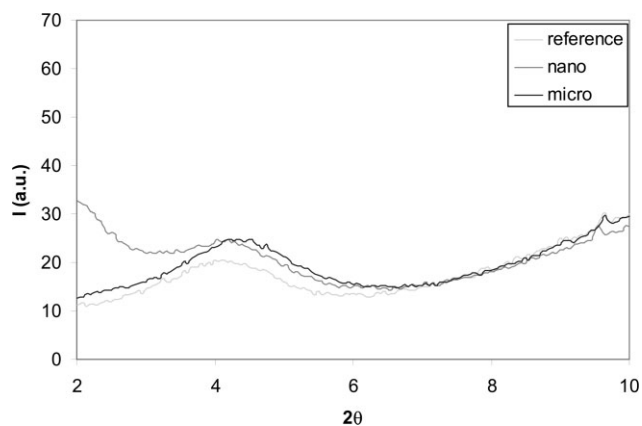
Figure 2 WAXS profiles of PU microcomposite and nanocomposite elastomers are compared with that of the reference pristine PU. Angular values are used to estimate the clay platelets and PU crystalline phases spacing by using the Bragg law. For the given source, wavelength Cu–Kα = 1.5418 Å, $d = nx$ wavelength/2sin θ.

1 h at high shear, the dispersion mixed for only 5 min still contained aggregates of undispersed clay.

Both wide angle X-ray scattering (WAXS) analysis and transmission electron microscopy (TEM) were carried out to investigate the degree of clay dispersion in the final PU elastomers, because these two techniques are complementary. X-ray diffraction is very useful to provide a quantitative measurement of clay intragallery spacing but cannot give any information about the dispersion homogeneity, which can be instead evaluated by means of TEM. On the other hand, due to its extremely high resolution, TEM only probes a very small volume while X-ray diffraction is representative of the whole composite.

In a previous publication,[1] SAXS analysis showed nearly complete clay exfoliation in the PU elastomer prepared with the polyol dispersion obtained after long mixing time.

In Figure 2, the WAXS curve corresponding to this sample shows a shoulder at very low angle, followed by a peak at 21 Å. This shoulder at low angle is due to the presence of some intercalated clay together with the exfoliated platelets, confirming the previous SAXS results.[1] The comparison with the curve obtained from the unmodified PU elastomer suggests that peaks at higher angle are due to the polymer crystallinity. The WAXS profile of the polyurethane elastomer prepared using the poorly dispersed polyol-clay mixture shows a peak at 20–21 Å, similar to that of the unmodified PU but slightly more intense and shifted to a higher angle. The pure clay spacing is 18 Å[1,10], and the peak observed is due to the superimposed reflections from polymer crystal segments and from undispersed clay.

The TEM micrographs of the elastomer prepared from the well-dispersed polyol-clay mixture in Figure 3 show that the material structure is made by exfoliated clay homogeneously dispersed in the PU matrix. Although some groups of widely spaced clay platelets ("tactoids," in the literature[4,12–15]) are observed at high magnification, this material can be defined a "nanocomposite."

The TEM micrographs in Figure 4 confirm the WAXS analysis results, showing aggregates of clay within the polyurethane matrix and no exfoliation for the elastomer prepared using the poorly dispersed polyol-clay mixture. Because of the lack of clay dispersion at nanoscale level, this material is classified as "microcomposite."
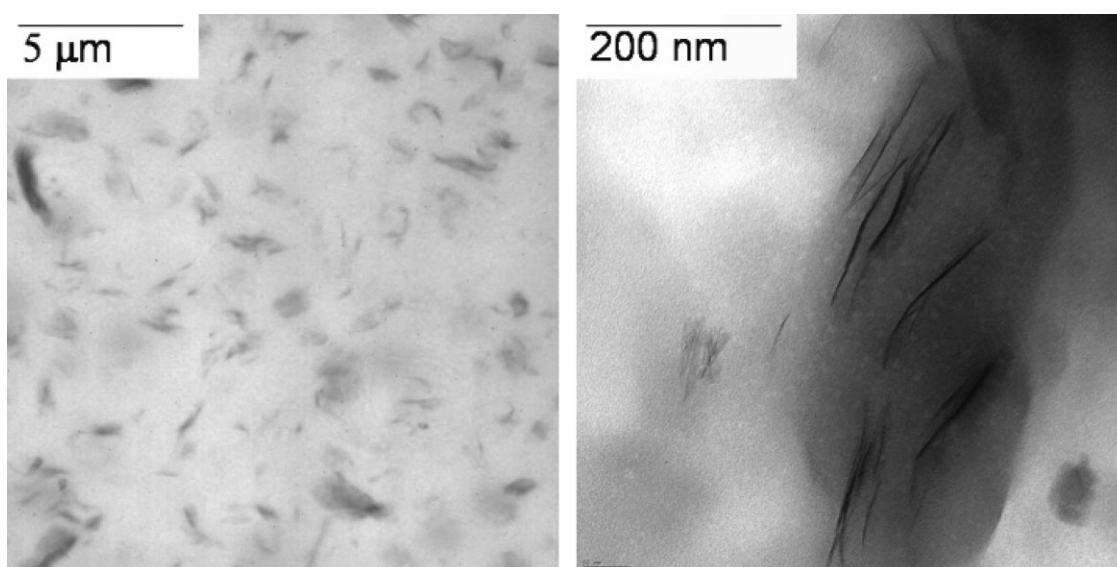

Figure 3 TEM micrographs of the PU elastomer obtained from the well dispersed polyol-clay mixture. Exfoliation of the clay occurs producing a nanocomposite PU-clay elastomer. At high magnification, clay tactoids can be observed.
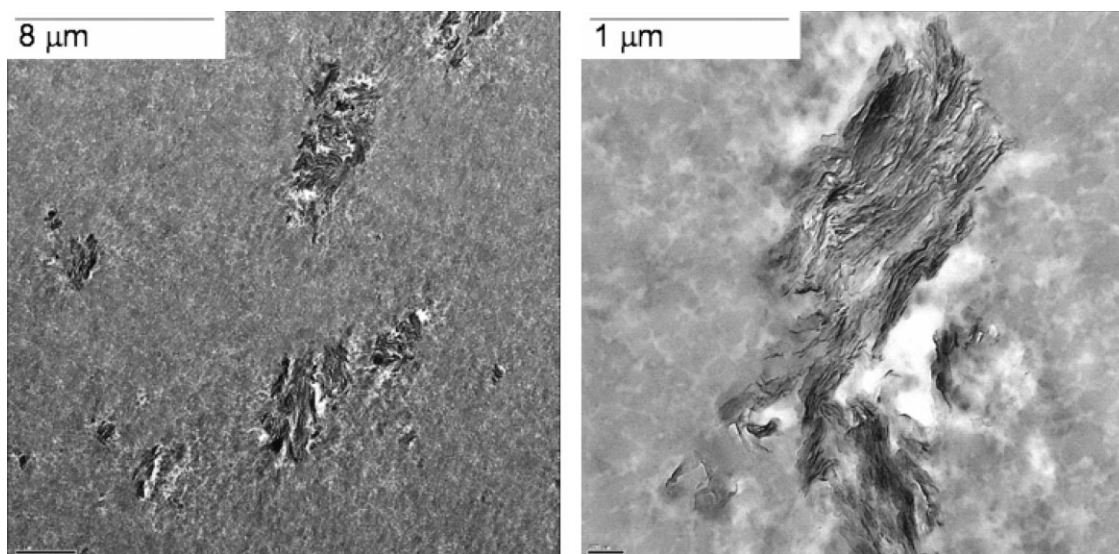
Figure 4 TEM micrograph of PU elastomer obtained from the poorly dispersed polyol-clay mixture.

Differential scanning calorimetry

The DSC curves in Figure 5 present a shoulder at $-65°C$ due to the polyurethane soft segment glass transition (T_g). Although the shoulder in the DSC graph lacks a clear baseline, a peak at a similar temperature, corresponding to the glass transition, has also been measured by means of DMTA (see below). Two endothermic (T_1 and T_2) peaks can be observed at 90°C and 130°C in the pure polymer while the clay containing materials show only a peak at 90°C. Similar results were obtained in the investigation of PU-clay nanocomposites DSC spectra by Finnigan et al.[2] and have been explained as a result of disordering of nonideally packed hard segments in which each endothermic peak corresponds to a specific hard segment length population. The peak at 90°C possibly corresponds to the glass transition of the hard block. That at 130°C instead can be related to the loss of crystallinity of the hard block and to the relaxation of the hard block segments by disruption with annealing temperature of intramolecular Van der Vaal forces, as shown by previous work on polyurethane materials.[16]
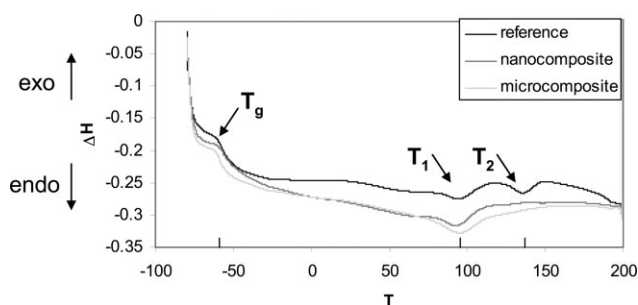
The disappearance of the peak at 130°C in the clay containing materials may be due to inhibition of hard block relaxation, due to the tethering of clay to the PU chains (Fig. 6), as observed in the research work of Pattanayak et al.[17] and, partially, to the confinement of hard block segments within clay interplatelets galleries when intercalation occurs.

Although the hydrogen bonding between hydroxyl groups in the Cloisite 30B modifying reagent and the polyurethane is still debated in the literature,[18] the investigation of this phenomenon by means of infra-red spectroscopy is beyond the scope of the present work. Further evidence of the relation between the DSC peaks at high temperature and
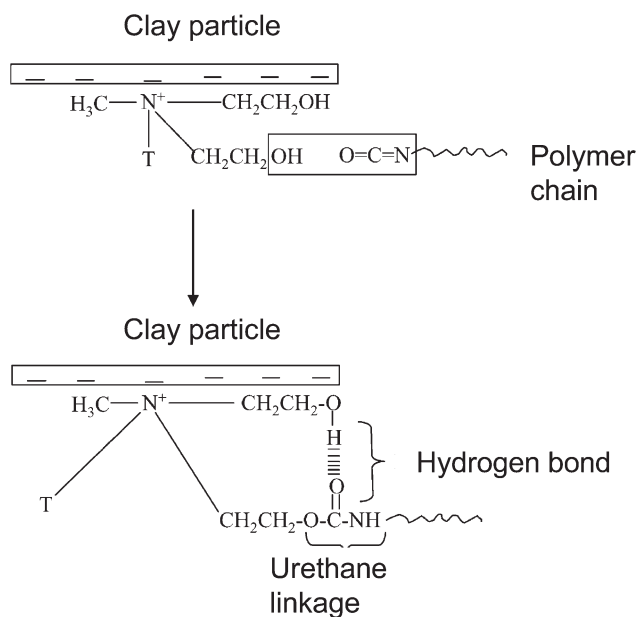

Figure 5 DSC curves for the investigated materials, resulting from the first heating cycle.

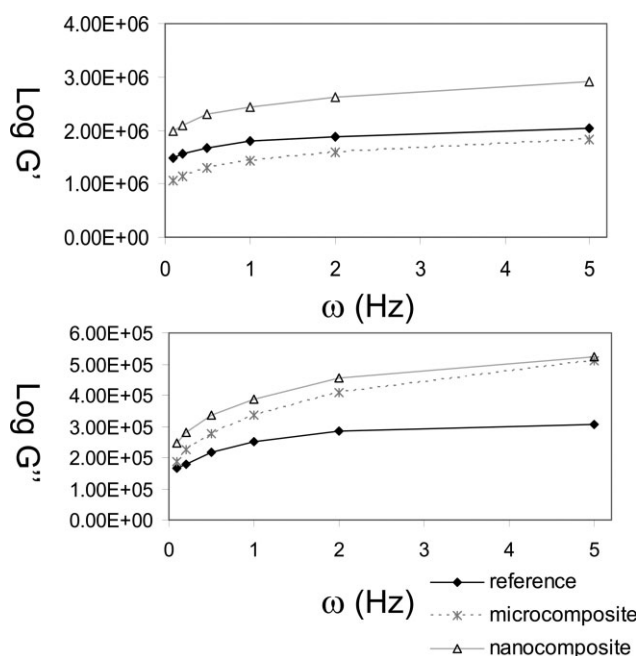**Figure 6** Hydrogen bonding by clay-tethered polyurethane chain.[17]

Figure 7 Frequency sweep oscillatory test results for nanocomposite, microcomposite, and pristine polyurethane.

the PU hard segment assembly is that no peaks appeared in the range 100–200°C for any of the three materials when a second thermal cycle was performed. This occurred because the order of hard segments was destroyed by the annealing process.

Rheological and mechanical properties

The frequency sweep oscillatory test results for all the investigated materials are presented in Figure 7. The loss modulus (G'') presents very similar values at low frequency for each set of data; at higher frequencies, G'' for clay containing materials slightly increases due to the resistance to flow imposed by hydrogen bonding between the Cloisite30B quaternary ammonium and tethered hard segments (see Fig. 6). The higher value for the exfoliated material can be explained by a stronger interaction between polymer and clay due to uniform nanoscale dispersion and much larger surface area of clay particles.

The storage modulus G' presents an improvement for the nanocomposite when compared with the pure polymer, whereas for the microcomposite, G' is initially lower and converges to the values of reference materials as the frequency increases.

The softness of the microcomposite material, measured by the low value of the storage modulus G' at low frequency, is possibly due to the presence of aggregates of clay; those have negligible interaction with the PU matrix and are detrimental for the mechanical properties. The material softness could also be partially attributed to the tethering reaction

between NCO groups and Cloisite 30B organomodifier, which competes with that of the chain extender. However, a chemical reaction between the OH-group of the clay and the isocyanate, which would affect the final molecular weight (and mechanical properties) of the polyurethane, is of minor importance when compared with the reaction with the polyol, due to the very low clay percentage.

The higher value of G' for the nanocomposite suggests that the exfoliated clay platelets may have some physical interactions or entanglements due to interplatelet association. That platelets self-assemble into a continuous "house of cards structure" is reported in other research work on nanodispersion;[19–21] but for the PU-clay nanocomposites, investigated TEM evidence shows only a local short-range platelets association into tactoids. It can be concluded that although the formation of tactoids is a relevant characteristic for these materials,[1,18] the enhancement of G' for the nanocomposite can be explained by the exfoliated clay hindering the polymer chains, rather than by percolation.

Tensile measurements (Table I) were conducted to support the observations on the storage modulus from the rheological test, because G' is directly related to the Young's modulus E.

The PU-clay microcomposite obtained with low degree of clay dispersion in the polyol, showed a lower modulus than the unmodified PU and a lower resistance (i.e., less elongation) since cracks, related to inhomogeneities caused by clay clusters, led to earlier breaking than the unmodified polymer. The high degree of exfoliation in the nanocomposite PU instead led to a significant improvement of the modulus and less reduction of the displacement at maximum load than the composite material. At high load, the polymer chains' mobility (and consequently the material elongation) was affected by the tethered clay but the exfoliated structure prevented cracks caused by the undispersed clay.

The effect of clay nanodispersion on the polymer chain mobility (and on phase transitions of the material) as a function of temperature has been evaluated by means of DMTA, performing a temperature sweep at constant frequency. This technique is more sensitive to the phase transitions than DSC and the

TABLE I
Values of Young's Modulus and Maximum Elongation from Tensile Tests

	Young's Modulus E (MPa)	Displacement at max. load (mm)
Pure PU	0.706 ± 0.089	310.4
PU microcomposite (5 min mix)	0.461 ± 0.030	119.2
PU nanocomposite (1 h mix)	0.863 ± 0.043	201.3

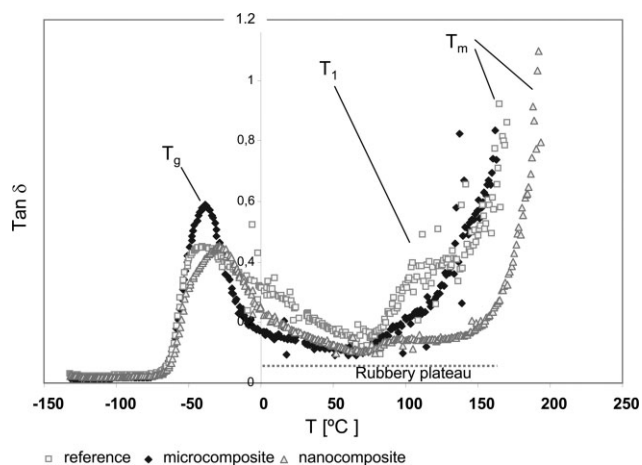**Figure 8** Tan δ versus temperature for the materials investigated. The curves show peaks associated to phase transitions of the material. It can be observed a slightly higher value of T_g and an extended rubbery plateau for the nanocomposite.

two can be regarded as complementary. With the use of DMTA, phase transitions can be evaluated by peak values of tan δ.

In Figure 8(a), peak at $\sim -40°C$ corresponding to the soft domains phase transition (T_g) can be observed for the microcomposite material and the pure polyurethane. For the nanocomposite material, this transition occurs at slightly higher temperature due to lower polymer chain mobility as an effect of the interaction with PU hard blocks and tethered platelets of exfoliated clay. This is followed by a rubbery plateau between the base of the peak corresponding to the T_g and the melting temperature. The rubbery plateau is important to define the material response to the annealing temperature and corresponds to the viscoelastic regime. The plateau in Figure 7 ends to $\sim 130°C$ for both the microcomposite and the pristine PU, whereas it is extended up to $\sim 170°C$ for the nanocomposite material. This extended viscoelastic regime can be explained by the effect of nanodispersion that enhances the material thermal stability[1] and preserves its mechanical properties at higher temperature. A shoulder at $\sim 90°C$ of the tan δ curves within the viscoelastic region can be observed for all the materials. Such variation corresponds to the T_1 peak observed in the DSC curves. This shoulder is more pronounced for the pure PU and is possibly related to the two peaks at 90°C and 130°C shown in the DSC graph in Figure 5, which results as a larger shoulder in the tan δ curve.

Fire properties

In previous work, it was shown that polymer-clay nanocomposites can be useful for the development of new flame-retardant materials. The current inves-

tigation relates the UL94 test results to the rheology of the materials investigated.

The PU-microcomposite material obtained from a polyol-clay dispersion mixed for a short time dripped heavily upon ignition with rapid extinction of the flame and ignition of the underlying cotton wool by the burning fragments [Fig. 9(a)]. This behavior was classified as a V-2 ranking according to ASTDM D3801, similar to the unmodified PU reported previously.[1] For the PU nanocomposite material, no dripping occurred initially, but the flame eventually propagated up to the top of the specimen leading to an unclassified ranking [Fig. 9(b)].

Similar conclusions from the UL 94 tests were made by comparing the unmodified PU and the nanocomposite material in the previous work.[1] In this investigation, it is important to stress that both materials shown in Figure 9 contain clay, which can potentially lead to char formation upon combustion, and they are differentiated solely by the level of clay dispersion.
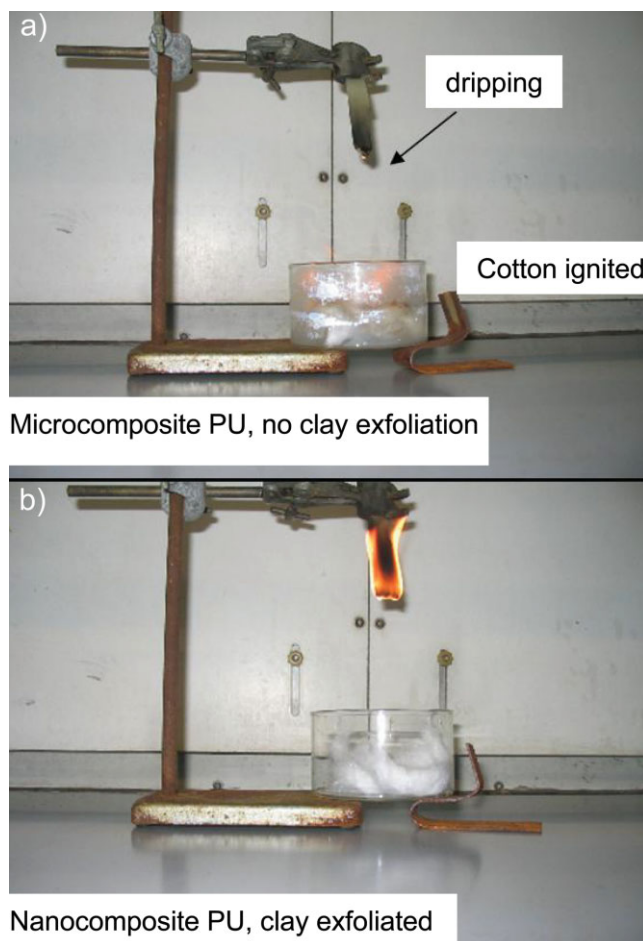

Figure 9 UL94 test for (a) microcomposite and (b) nanocomposite polyurethane elastomer. Clay nanodispersion prevents dripping for the composite having an exfoliated structure. [Color figure can be viewed in the online issue, which is available at www.interscience.wiley.com.]

The presence of an exfoliated clay structure enhances the structural stability of the nanocomposite material at high temperature (shown by the tan δ curve Fig. 8) and leads to the suppression of dripping during the UL94 tests. Although the flame temperature is higher than that of the nanocomposite viscoelastic region, melting is initially prevented by quick formation of char on the surface and propagation of the flame to the adjacent position. Upon ignition, char-forming reactions occur in the PU nanocomposites owing to the barrier formed by the nanodispersed clay to the diffusion of both the oxygen into the polymer matrix and the polymer degradation products towards the gas phase.[1] Such a barrier effect causing rapid char formation is lacking in the microcomposite material, due the poor dispersion of the clay. Melting and consequent dropping of the nanocomposite specimen occurs only few seconds after the flame has reached the clamp at the top. This behavior is related both to the char layer heat insulation and to the enhancement of mechanical properties at high temperature by the clay nanodispersion.

The prevention of dripping is known to be necessary to avoid spreading fire by the burning drops and can be considered a major advantage of the nanocomposite materials. On the other hand, the decreased melt flow results in increasing conversion of the material when fire is applied (i.e., charring and propagation of flame). The stabilization of the material at high temperature by its nanocomposite structure, while a distinct advantage to ensure barrier properties, can be at the same time disadvantageous for passing flammability tests.

CONCLUSIONS

The dispersion of organoclay in the polyol proves to have an effect both on phase separation and mechanical properties of the final polyurethane elastomers. Phase separation is enhanced by the presence of the clay and the tethering of hard segments to clay platelets, and improves the resistance of the material to shear stress. The results of rheological and tensile tests conducted at room temperature show an enhancement of composite material storage (G') and elastic (E) modulus with clay exfoliation. The same mechanism enhances also the thermal stability of the nanocomposite material, which retains viscoelastic behavior at higher temperatures than the pristine polyurethane. In the PU-clay microcomposite elastomer, the poor dispersion of the filler is detrimental for the mechanical properties, leading to lower mod-

ulus and earlier breaking than unmodified PU during the tensile test due to the initiation of crazes by the clay aggregates. Exfoliation of the clay and the consequent enhancement of viscoelasticity with temperature also affect the fire properties of the nanocomposite material. Char develops quickly upon ignition in the nanocomposite due to a barrier effect of the exfoliated clay; both the char layer and reduced mobility of polymer chains prevent the flow and dripping caused by polymer melting. Dripping instead occurs for the microcomposite material, which shows the same fire properties of the pure PU.

References

1. Berta, M.; Lindsay, C.; Pans, G.; Camino, G. Polym Degrad Stab 2006, 91, 1179.
2. Finnigan, B.; Martin, D.; Halley, P.; Truss, R.; Campbell, K. Polymer 2004, 45, 2249.
3. Pattanayak, A.; Jana, S. C. Polymer 2005, 46, 5183.
4. Ranade, A.; D'Souza, N. A.; Gnade, B. Polymer 2002, 43, 3759.
5. Gelfer, M.; Song, H.; Lizhi, L.; Avila-Orta, C.; Yang, L.; Mayu, S.; Hsiao, B. S.; Chu, B.; Rafailovich, M.; Tsou, A. Polym Eng Sci 2002, 42, 1841.
6. Krishnamoorti, R.; Yurekli, K. Curr Opin Colloid Interface Sci 2001, 6, 464.
7. Kim, B. K.; Seo, J. W.; Jeong, H. M. Eur Polym J 2003, 39, 85.
8. Madbouly, S. A.; Otaigbe, J. U. Proceedings of The XV International Congress on Rheology: The Society of Rheology 80th Annual Meeting, Monterey (California), 2008, pp 812–814.
9. Samyn, F.; Bourbigot, S.; Jama, C.; Bellayer, S. Polym Degrad Stab 2008, 93, 2019.
10. Huang, W.; Han, C. D. Polymer 2006, 47, 4400.
11. Meng, X.; Du, X.; Wang, Z.; Bi, W.; Tang, T. Compos Sci Technol 2008, 68, 1815.
12. Yoon, P. J.; Hunter, D. L.; Paul, D. R. Polymer 2003, 44, 5323.
13. Tidjani, A.; Wald, O.; Pohl, M.-M.; Hentschel, M. P.; Schartel, B. Polym Degrad Stab 2003, 82, 133.
14. Rajeev, R. S.; Harkin-Jones, E.; Soon, K.; McNally, T.; Menary, G.; Armstrong, C. G.; Martin, P. J. Mater Lett 2008, 62, 4118.
15. Calcagno, C. I. W.; Mariani, C. M.; Teixeira, S. R.; Mauler, R. S. Polymer 2007, 48, 966.
16. Saiani, A.; Daunch, W. A.; Werbeke, H.; Leenslagand, J. W.; Higgins, J. S. Macromolecules 2001, 34, 9059.
17. Pattanayak, A.; Jana, S. C. Polymer 2005, 46, 3275.
18. Chun, B. C.; Cho, T. K.; Chong, M. H.; Chung, Y. C.; Chen, J.; Martin, D.; Cieslinski, R. C. J Appl Polym Sci 2007, 106, 712.
19. Luckham, P. F.; Rossi, S. Adv Colloid Interface Sci 1999, 82, 43.
20. Mele, P.; Marceau, S.; Brown, D.; Alberola, N. D. Comptes Rendus Mecanique 2005, 333, 155.
21. Burgentzle, D.; Duchet, J.; Gerard, J. F.; Jupin, A.; Fillon, B. J Colloid Interface Sci 2004, 278, 26.